Supporting Information

One-step electrodeposition of Cu-CoP_3 for efficient electrochemical nitrate reduction to ammonia

Chun Liu, [a] Juhong Miao, [a] Man Qiao, [a] Dongdong Zhu, *[ab] Gao Chen, [a] Dazhi Yao *[c] and Dongsheng Geng *[a]

[a] School of Chemistry and Materials Science, Jiangsu Key Laboratory of New Energy Devices and Interface Science, Nanjing University of Information Science and Technology, Nanjing 210044, China. E-mail: dd.zhu@nuist.edu.cn, dgeng@nuist.edu.cn

[b] Key Laboratory of Advanced Energy Materials Chemistry (Ministry of Education), Nankai University, Tianjin 300071, China

[c] 1 Technology Court, CSIRO Mineral Resources, Pullenvale, QLD 4069, Australia. E-mail: dazhi.yao@csiro.au

1 Experimental section

1.1 Materials

Sodium citrate ($C_6H_5O_7Na_3$), salicylic acid ($C_7H_6O_3$), sodium nitroferricyanide dihydrate ($C_5FeN_6Na_2O\cdot 2H_2O$), phosphoric acid (H_3PO_4), and sodium hypophosphite monohydrate ($NaH_2PO_2\cdot H_2O$) were purchased from Aladdin Ltd. (Shanghai, China). Potassium hydroxide (KOH), ammonium chloride (NH_4Cl), sulfanilamide ($C_6H_8N_2O_2S$), sodium hypochlorite (NaClO), potassium nitrite (KNO_2), and N-(1-naphthyl) ethylenediamine dihydrochloride ($C_{12}H_{14}N_2\cdot 2HCl$) were purchased from Macklin Inc. (Shanghai, China). Ammonium fluoride (NH_4F), cobalt(II) nitrate hexahydrate ($Co(NO_3)_2\cdot 6H_2O$), ethanol absolute (C_2H_5OH), copper(II) sulfate pentahydrate ($CuSO_4\cdot 5H_2O$), potassium nitrate (KNO_3), hydrochloric acid (HCl), and sodium hydroxide (NaOH) were purchased from China National Pharmaceutical Group Corp. All reagents in this work were used without further purification. Ultrapure water (Millipore Milli-Q grade) with a resistivity of 18.25 MΩ was used in all experiments.

1.2 Preparation of Cu-CoP_3, CoP_3, and Cu

In brief, a piece of Ni foam (2 cm × 3 cm) was ultrasonicated in 2.0 M HCl, ethanol absolute, and Milli-Q water for 8 min, respectively. Firstly, 3.0 mmol of $Co(NO_3)_2\cdot 6H_2O$, 0.1 mmol of $CuSO_4\cdot 5H_2O$, 63.0 mmol of NH_4F and 7.0 mmol of $NaH_2PO_2\cdot H_2O$ were dissolved in an electrolytic cell containing 50 ml of deionized water to form a transparent solution by magnetic stirring. A standard three-electrode cell was employed for electrodeposition, using the above mixed solution as the electrolyte. The pretreated Ni foam, a platinum sheet, and a Hg/HgO electrode serve as the working electrode, counter electrode, and reference electrode, respectively. Cu-CoP_3 was prepared by electrodeposition at a constant voltage of −4 V for 40 min on an electrochemical workstation. All the potentials used during electrodeposition are measured against the reversible hydrogen electrode (RHE). For comparison, CoP_3 was prepared by the same method without the use of $CuSO_4\cdot 5H_2O$. Similarly, Cu was prepared without the use of $Co(NO_3)_2\cdot 6H_2O$.

1.3 Characterizations

The X-ray diffraction (XRD) patterns of the samples were obtained on Smart Lab/3 kW with Cu Kα radiation. The morphology of the samples was characterized by field emission scanning electron microscopy (FESEM, Zeiss Gemini SEM 300) equipped with an energy dispersive spectrometer (EDS) and transmission electron microscopy (TEM, JEOL JEM-2100F). X-ray photoelectron spectroscopy (XPS) measurements were carried out on an ESCALab250 using Al Kα radiation, and the working voltage is 12.5 KV. The binding energy was calibrated to the C 1s peak of 284.8 eV.

1.4 Electrochemical measurements

All electrochemical measurements reported in this study were performed on a CHI 760E electrochemical workstation (Chenhua, Shanghai). The electrocatalytic performance of the obtained catalysts was evaluated by using a two-chamber H-type cell with a three-electrode system, in which the cathode chamber was separated from the anode chamber through a cation exchange membrane (Nafion 117). The Nafion 117 was pretreated according to the reported literature.[1] The prepared catalyst was used as the working electrode, while Pt sheet and Hg/HgO electrode served as the counter and reference electrodes, respectively, and 1.0 M KOH solution (40 mL) containing 0.1 M KNO_3 was used as electrolyte. All potentials were recorded against the reversible hydrogen electrode (RHE), and no IR correction was applied for the presented results. Linear sweep voltammetry (LSV) was performed at a scan rate of 10 mV s^{-1}. Potentiostatic tests were conducted in 1 M KOH containing 0.1 M NO_3^- at various potentials for 1.0 h with a stirring rate of 1000 rpm.

1.5 Detection of ammonia

The NH_3 concentration was determined by indophenol blue spectrophotometry. Under alkaline conditions, ammonia nitrogen (NH_3/NH_4^+) reacts with sodium hypochlorite (NaClO) and phenolic compounds (phenol or salicylic acid) to produce the blue color indophenol blue in the presence of a sodium nitroferricyanide dihydrate catalyst. Firstly, 2.5 g of $C_6H_5O_7Na_3$ and 2.5 g of $C_7H_6O_3$ were dissolved in 50.0 mL of 1.0 M NaOH to prepare the colorant, noted as Reagent A. Reagent B was 0.05 M NaClO.

Dissolve 0.2 g of $C_5FeN_6Na_2O \cdot 2H_2O$ in 20 mL of ultrapure water to prepare the catalyst, noted as Reagent C. Secondly, the quantification process is as follows: take out a certain amount of electrolyte and dilute it to the detection range. Then take 2 mL of the diluted solution and add 2.0 mL of reagent A, 1.0 mL of reagent B and 0.2 mL of reagent C in turn, shake well to mix, and leave it for 2 hours away from light. Next, the UV-Vis absorbance was measured at a wavelength of 655 nm. The concentration-absorbance curve was calibrated using the standard NH_4Cl solution with concentrations of 0, 0.50, 1.00, 1.50, 2.00, and 2.50 ppm of 1.0 M KOH solution. Then the concentration of NH_3 product was calculated according to the absorbance and standard curve.

1.6 Detection of nitrite

The NO_2^- concentration was detected by the naphthalene ethylenediamine hydrochloride method. Under acidic conditions, nitrite will undergo diazotization with sulfanilamide, and then couple with N-(1-naphthyl) ethylenediamine dihydrochloride to form a rose-red azo dye. According to the intensity of its color, it is quantitatively determined by the spectrophotometric method. Firstly, 0.2 g $C_{12}H_{14}N_2 \cdot 2HCl$ and 4.0 g $C_6H_8N_2O_2S$ were dissolved in 50 mL of deionized water, to which 10 mL of H_3PO_4 (ρ=1.7 g/mL) was added to obtain a mixed solution. Secondly, the quantification process is as follows: the electrolyte sample was collected and diluted to the detection range. Then 40 μl of the color reagent was added into the 2.0 ml sample solution, mixed thoroughly and rested for 20 min at ambient conditions. Next, the UV-Vis absorbance was measured at a wavelength of 540 nm. The concentration-absorbance curve was calibrated using the standard KNO_2 solution with concentrations of 0, 0.50, 1.00, 1.50, 2.00, and 2.50 ppm of 1.0 M KOH solution. Then the concentration of NO_2^- product was calculated according to the absorbance and standard curve.

1.7 Calculations of faradaic efficiency (FE) and NH_3 yield

NH_3 FE = (8 × F ×V × C×A) / (M_{NH_3} × Q) × 100%

NO_2^- FE = (2 × F ×V × C×A) / ($M_{NO_2^-}$ × Q) × 100%

NH_3 yield = (C × V ×A) / (M_{NH_3} × S × t)

Where F is the Faraday constant (96485 C mol^{-1}), V is the volume of electrolyte in the H-cell cathode chamber (40 mL), C is the measured concentration of the diluted product, A is the dilution factor, M_{NH_3} is the molar mass of NH_3, $M_{NO_2^-}$ is the molar mass of NO_2^-, Q is the total quantity of applied electricity, S is the loaded area of catalyst (0.5 cm × 0.5 cm), t is the electrolysis time (1.0 h).

2 Supplementary Figures and Table

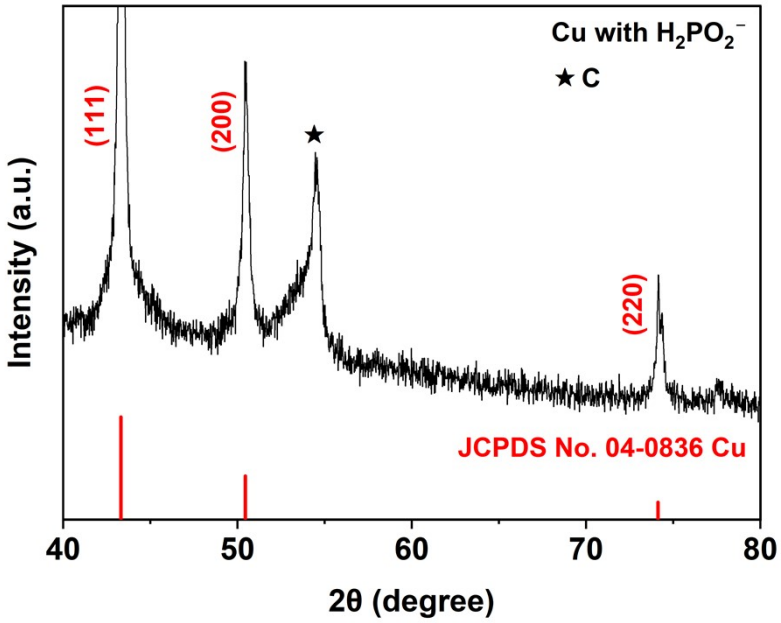

Figure S1. XRD pattern of the sample prepared via electrodeposition method in the electrolyte containing $CuSO_4 \cdot 5H_2O$, NH_4F and $NaH_2PO_2 \cdot H_2O$.

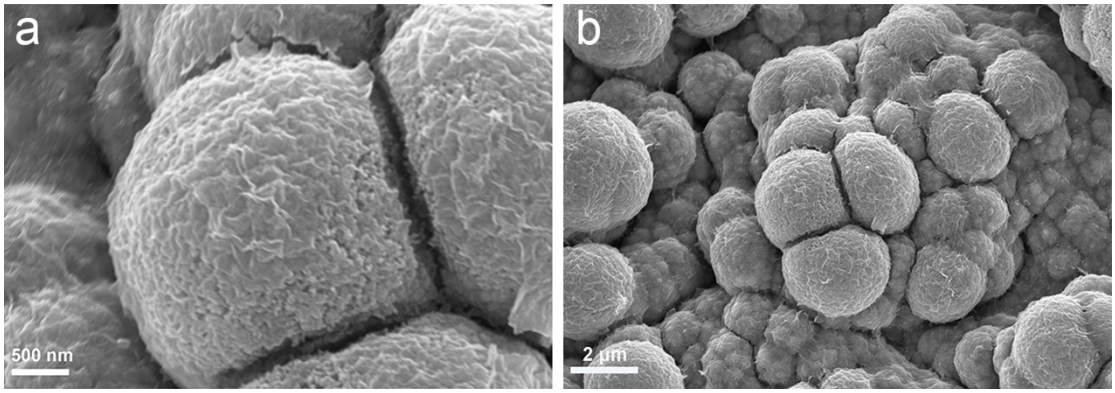

Figure S2. (a, b) SEM images of CoP_3 with different magnifications.

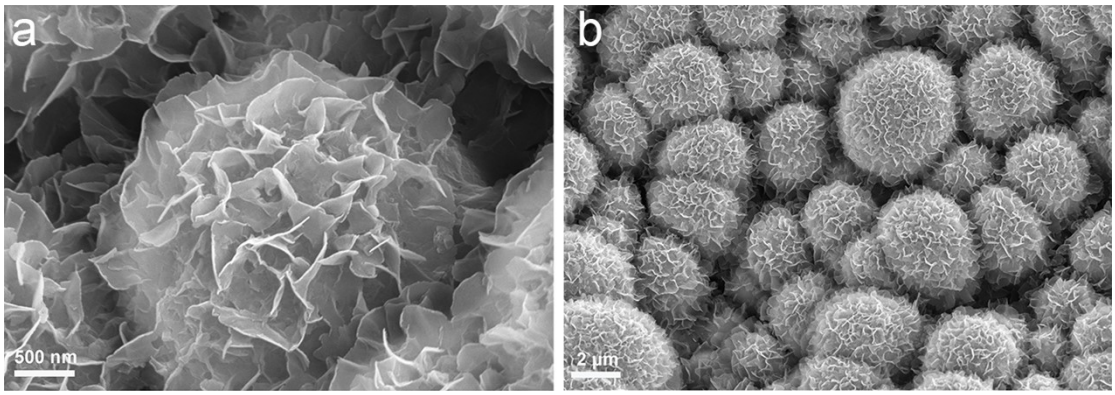

Figure S3. (a, b) SEM images of Cu-CoP_3 with different magnifications.

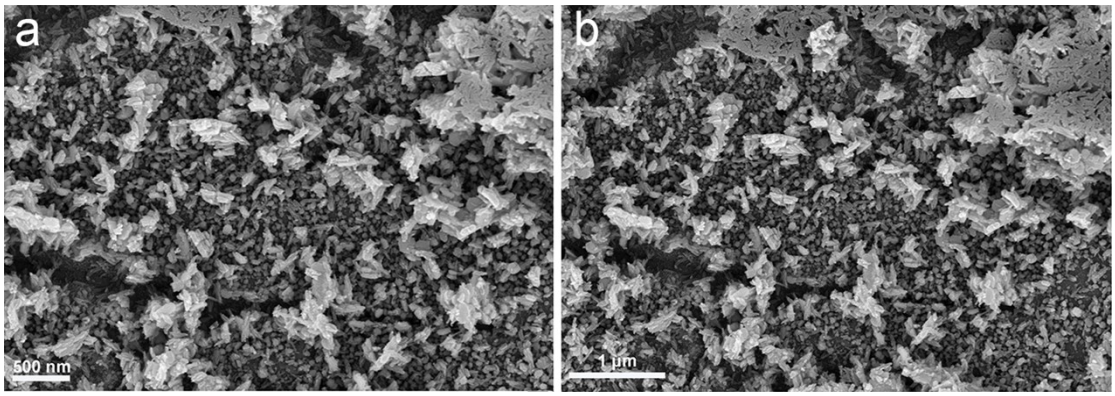

Figure S4. (a, b) SEM images of Cu with different magnifications.

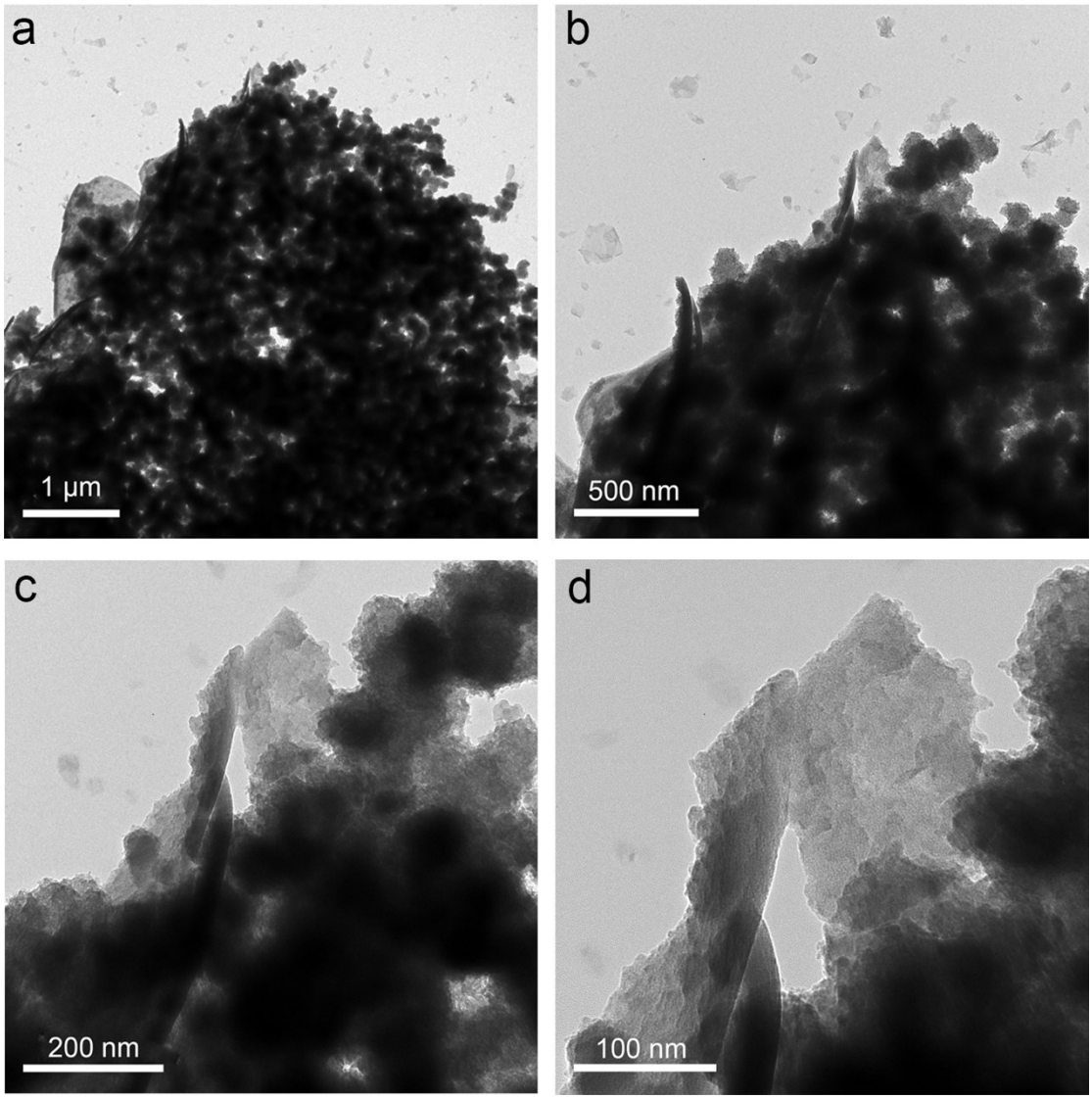

Figure S5. (a-d) TEM images of Cu-CoP_3 with different magnifications.

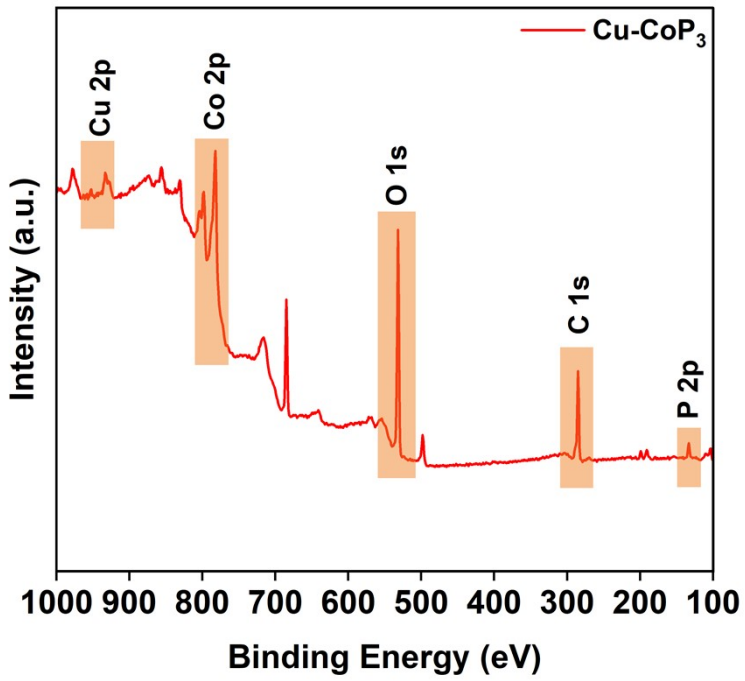

Figure S6. XPS survey spectrum of Cu-CoP_3.

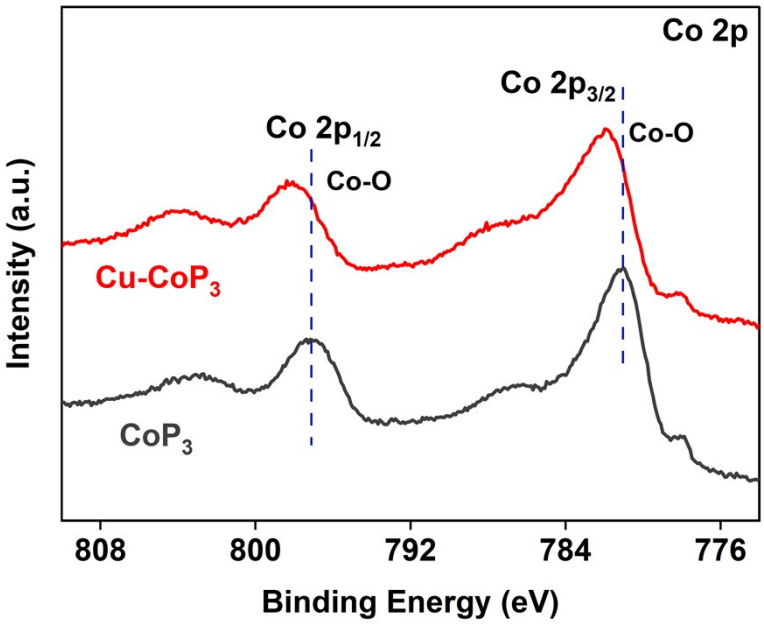

Figure S7. XPS Co 2p spectra of Cu-CoP_3 and CoP_3.

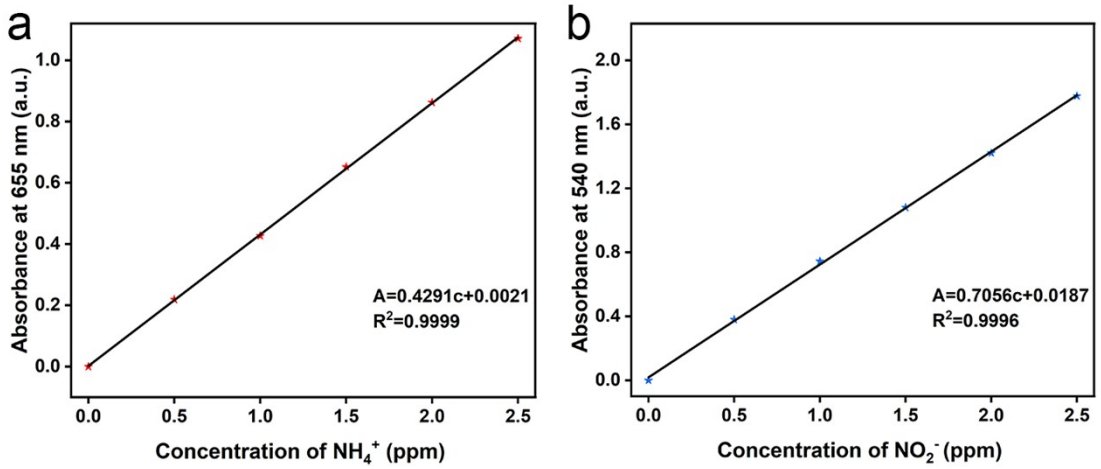

Figure S8. The concentration-absorbance calibration curves for (a) NH_4^+, and (b) NO_2^-.

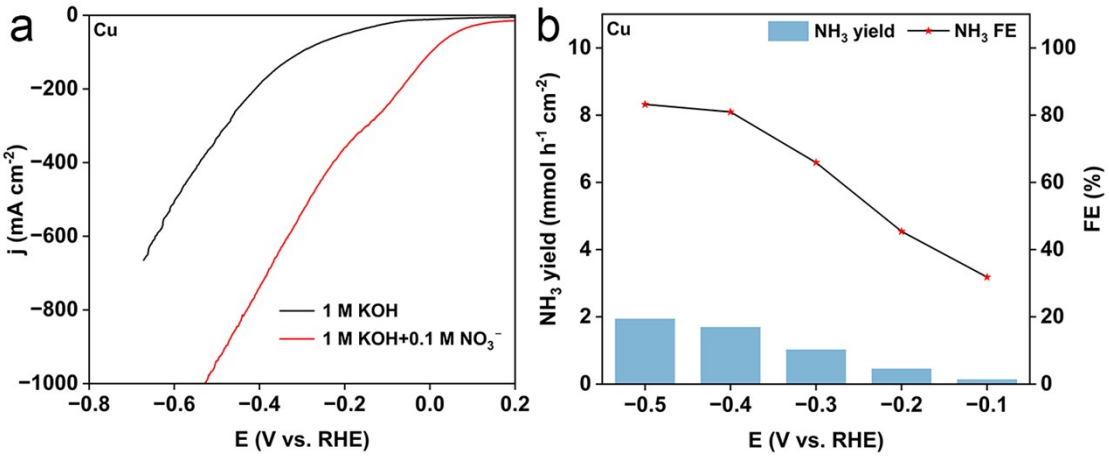

Figure S9. NH_3 yields and FEs of Cu tested at different applied potentials for 1.0 h in 1.0 M KOH with 0.1 M NO_3^-.

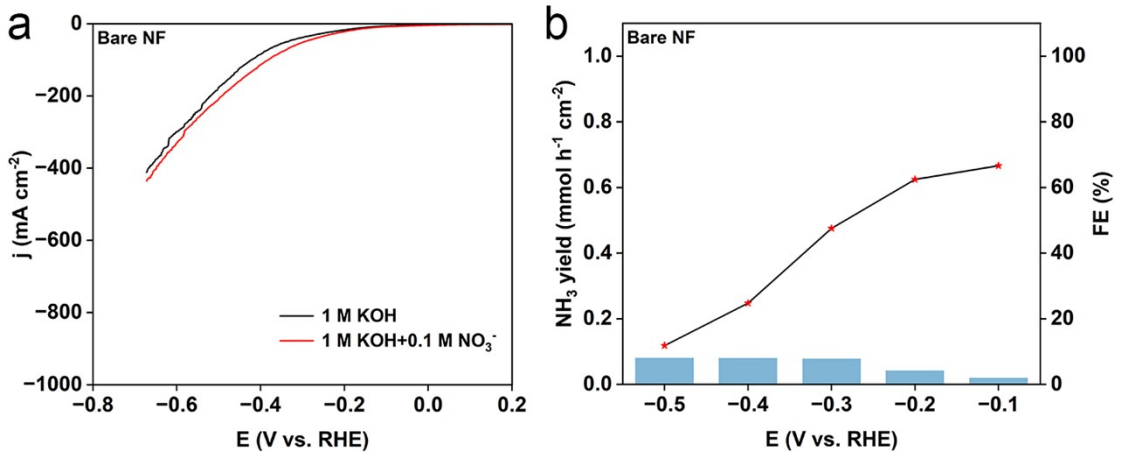

Figure S10. (a) LSV curves of bare NF in different electrolytes, (b) NH_3 yields and FEs of bare NF at different applied potentials.

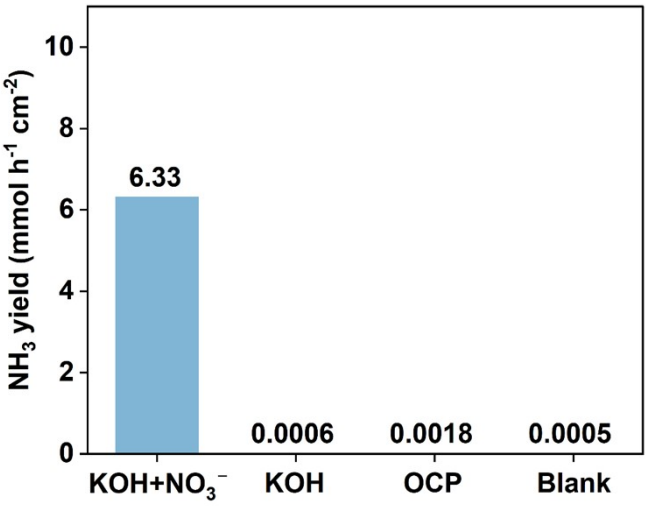

Figure S11. Comparison of NH_3 yields on Cu-CoP_3 under different test conditions.

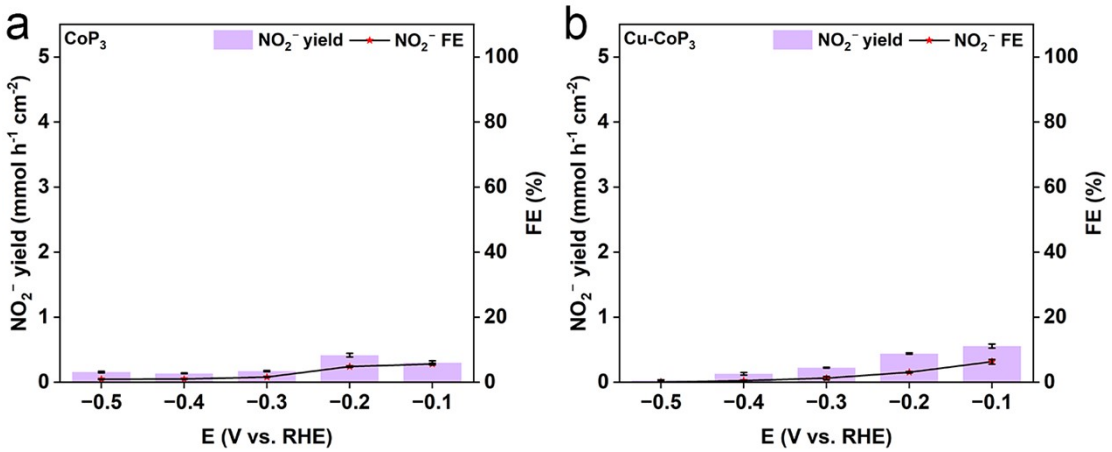

Figure S12. NO_2^- yields and FEs of (a) CoP_3, and (b) Cu-CoP_3 tested at different applied potentials in 1.0 M KOH with 0.1 M NO_3^-.

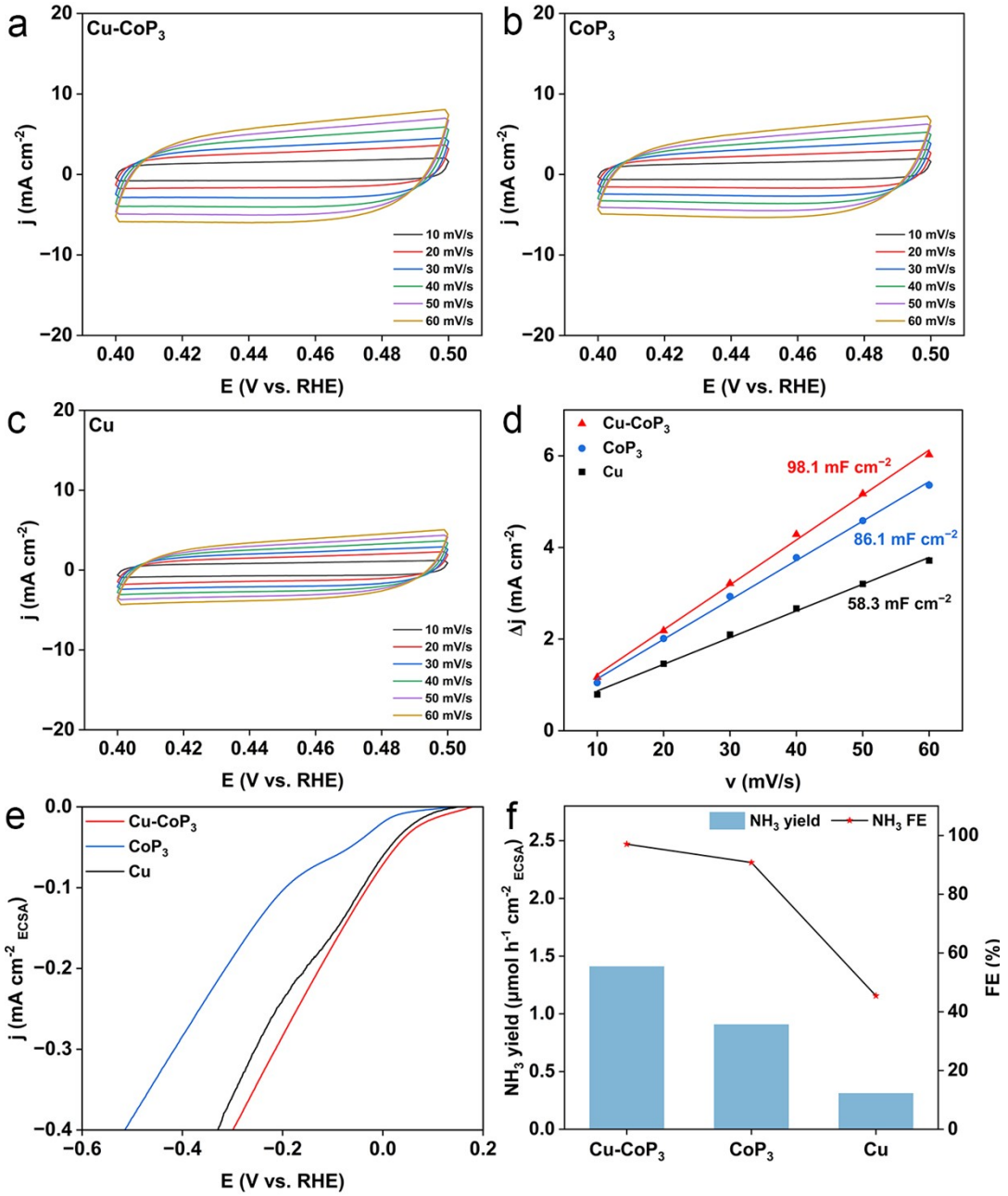

Fig. S13. ECSA measurements of (a) Cu-CoP_3, (b) CoP_3, and (c) Cu. (d) Double layer capacitance (C_{dl}) of the samples. (e) ECSA-normalized LSV curves of the samples in 1.0 M KOH with 0.1 M NO_3^-. (f) NH_3 FEs and ECSA-normalized NH_3 yields of the samples tested at −0.2 V *vs*. RHE in 1.0 M KOH with 0.1 M NO_3^-.

C_{dl} values are converted to electrochemical active surface area (ECSA) by the following equation: ECSA= C_{dl}/C_s. The specific capacitance(Cs) for a flat surface is generally in the range of 20-60 μF cm^{-2}, and here 40 μF cm^{-2} is used (*Angew. Chem. Int. Ed.*, 2014, 53, 14433). Therefore, ECSAs of Cu-CoP_3, CoP_3, and Cu are calculated to be 2452.5, 2152.5, and 1457.5 cm^2_{ECSA}, respectively.

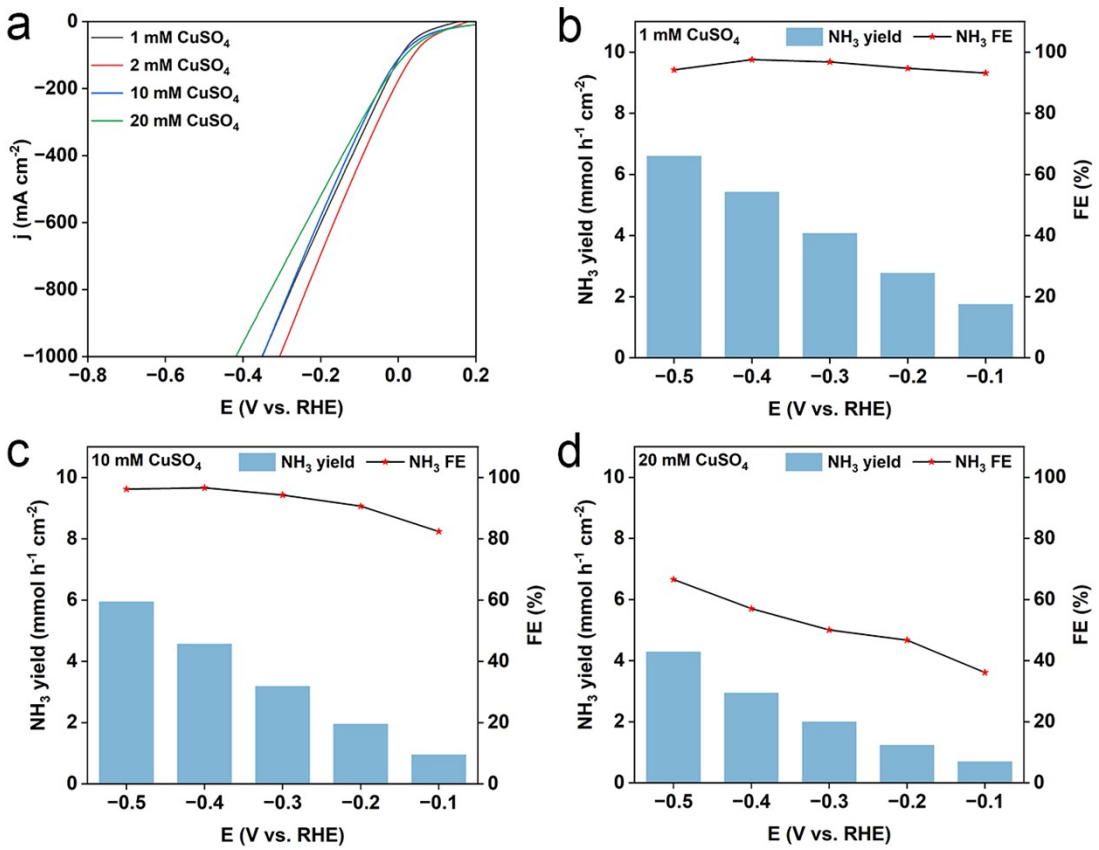

Figure S14. In 1.0 M KOH with 0.1 M NO_3^-, NO_3RR performance of Cu-CoP_3 samples prepared with different Cu content in the electrodeposition solution. (a) LSV curves of different Cu-CoP_3 samples, (b) NH_3 yields and FEs of Cu-CoP_3 sample prepared with 1 mM $CuSO_4$ in the electrodeposition solution, (c) NH_3 yields and FEs of Cu-CoP_3 sample prepared with 10 mM $CuSO_4$ in the electrodeposition solution, and (d) NH_3 yields and FEs of Cu-CoP_3 sample prepared with 20 mM $CuSO_4$ in the electrodeposition solution.

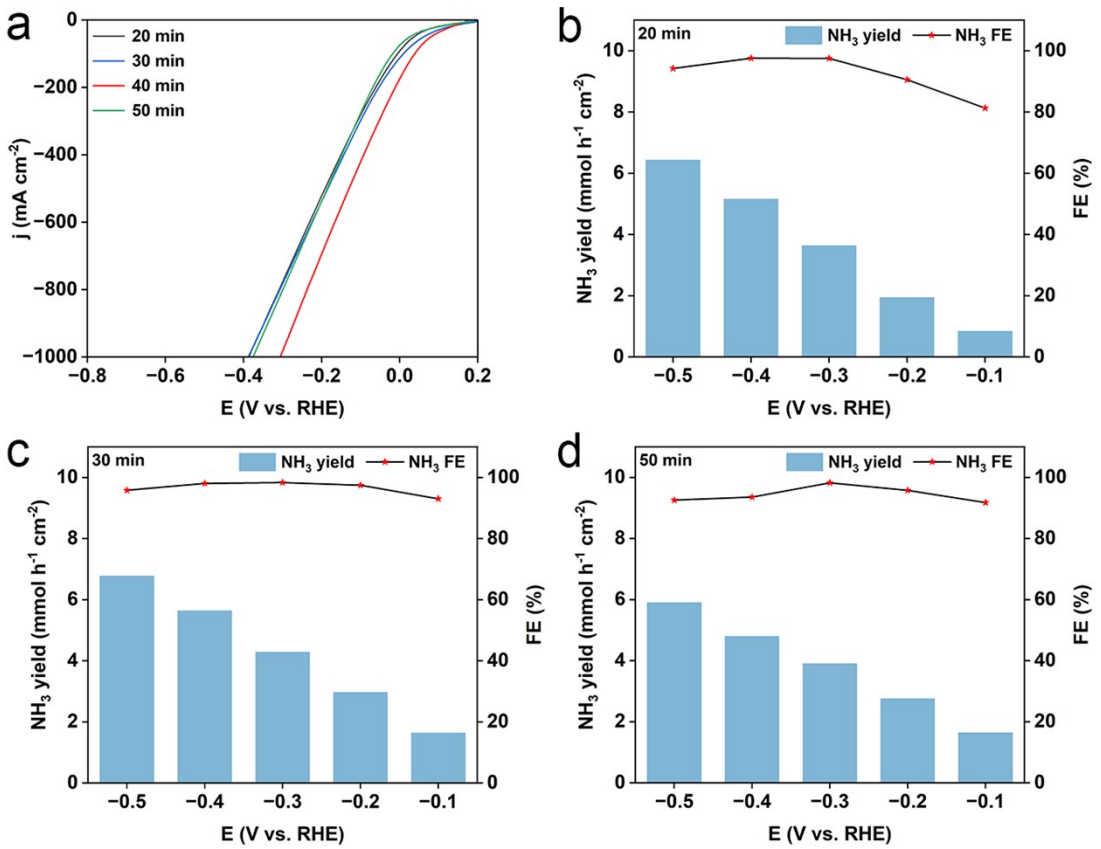

Figure S15. In 1.0 M KOH with 0.1 M NO_3^-, NO_3RR performance of Cu-CoP_3 samples prepared with different electrodeposition time. (a) LSV curves of different Cu-CoP_3 samples, (b) NH_3 yields and FEs of Cu-CoP_3 sample prepared with 20 min, (c) NH_3 yields and FEs of Cu-CoP_3 sample prepared with 30 min, and (d) NH_3 yields and FEs of Cu-CoP_3 sample prepared with 50 min.

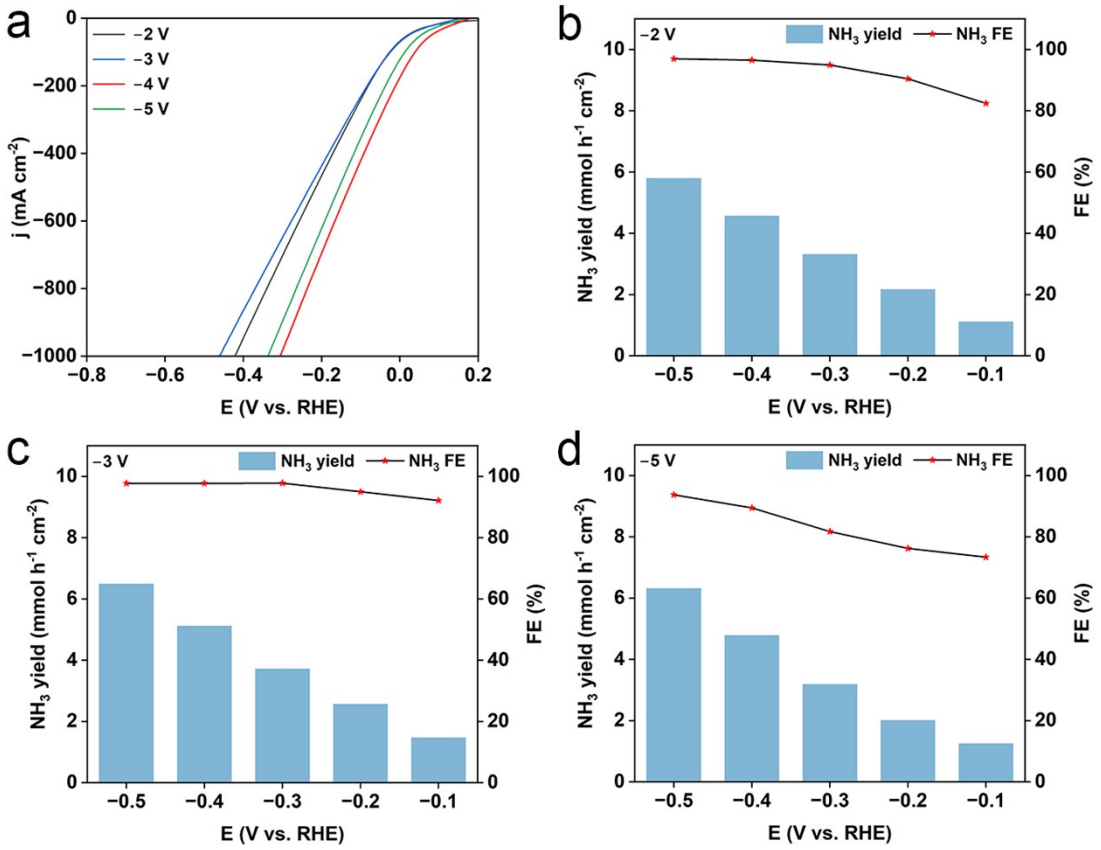

Figure S16. In 1.0 M KOH with 0.1 M NO_3^-, NO_3RR performance of Cu-CoP_3 samples prepared with different electrodeposition potential. (a) LSV curves of different Cu-CoP_3 samples, (b) NH_3 yields and FEs of Cu-CoP_3 sample prepared with −2 V, (c) NH_3 yields and FEs of Cu-CoP_3 sample prepared with −3 V, and (d) NH_3 yields and FEs of Cu-CoP_3 sample prepared with −5 V.

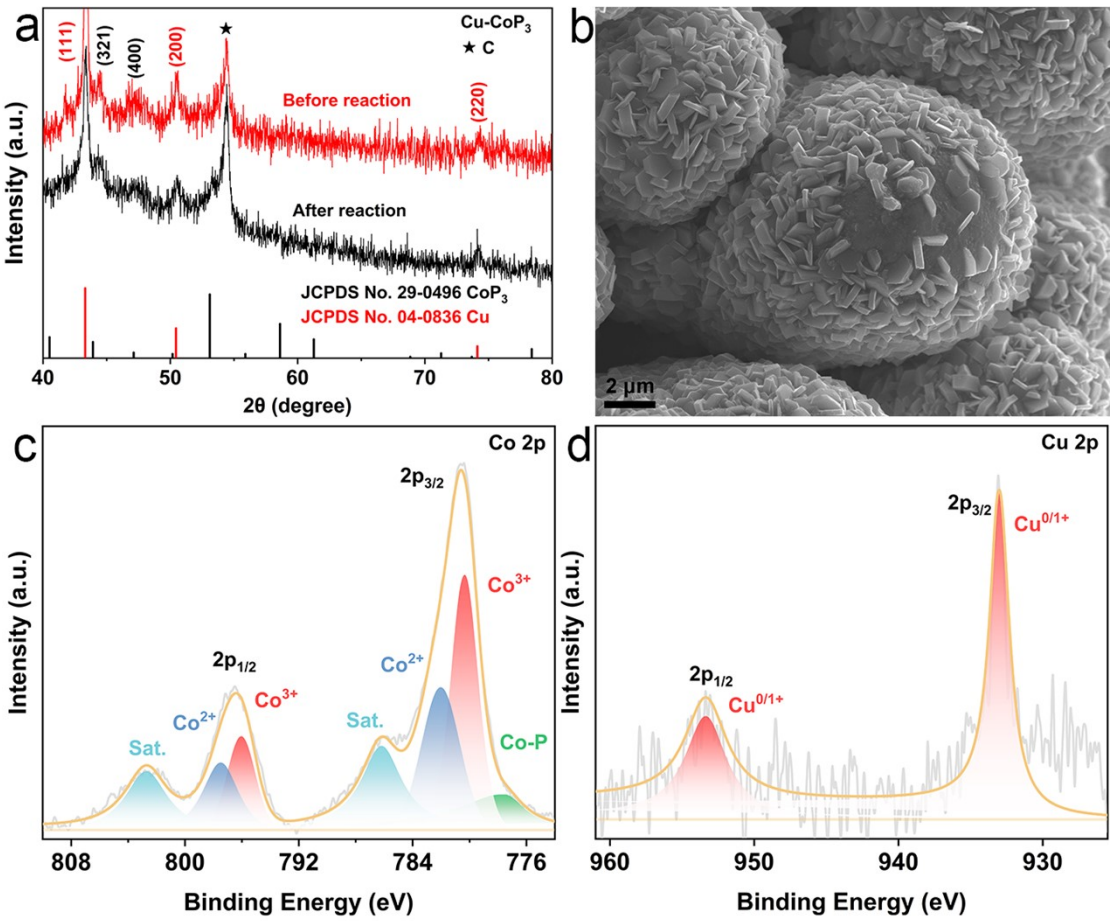

Figure S17. (a) XRD patterns of Cu-CoP_3 before and after NO_3RR cycling test. (b) SEM image of Cu-CoP_3 after NO_3RR cycling test. XPS spectra of Cu-CoP_3 after NO_3RR cycling test: (c) Co 2p, and (d) Cu 2p.

Table S1. Summary of the electrochemical NO_3RR performance of some representative electrocatalysts in alkaline electrolytes.

Catalyst	**Electrolyte**	**Potential (V vs. RHE)**	**NH_3 yield (mmol h^{-1} cm^{-2})**	**NH_3 FE (%)**	**Ref.**
Cu-CoP_3	**1 M KOH + 0.1 M NO_3^-**	**−0.4**	**6.33**	**99.1**	**This work**
NF/Ni_3N-Cu	1 M KOH + 0.1 M NO_3^-	−0.3	1.19	98.7	2
$Ni(OH)_x$/Cu	1 M KOH + 0.1 M NO_3^-	−0.25	3	92	3
W-O-CoP	1 M KOH + 0.1 M NO_3^-	−0.5	4.76	95.2	4
Sn-FeS_2	1 M KOH + 0.1 M NO_3^-	−0.5	0.929	96.7	5
R-CoCu@CF	1 M KOH + 0.1 M NO_3^-	−0.5	3.9	97.7	6
CuNi-LDHs	0.1 M KOH + 0.1 M NO_3^-	−0.4	0.161	94.65	7
CuNi-LDH@Cu_2O	1 M NaOH + 0.1 M NO_3^-	−0.4	4.42	97.8	8
Cr-CoO_x	1 M KOH + 0.1 M NO_3^-	−0.7	3.466	97.36	9
Cu/Cu_xO/ GDY	1 M KOH + 0.1 M NO_3^-	−0.8	1.5	99.8	10
Ni_1Cu SAAO	1 M KOH + 0.1 M NO_3^-	-0.3	0.84	100	11

References

1. G. Xu, X. Peng, C. Wu, S. Xi, H. Xiang, L. Feng, Z. Liu, Y. Duan, L. Gan, S. Chen, Y. Kong, Y. Ma, F. Nie, J. Zhao, X. Hai, W. Wei, M. Zhou, T. Wang, C. Yao, W. Zhou and H. Yan, *Nat. Commun.*, 2025, **16**, 3774.
2. X. Ouyang, W. Qiao, Y. Yang, B. Xi, Y. Yu, Y. Wu, J. Fang, P. Li and S. Xiong, *Angew. Chem. Int. Ed.*, 2025, **64**, e202422585.
3. W. Liu, M. Xia, C. Zhao, B. Chong, J. Chen, H. Li, H. Ou and G. Yang, *Nat. Commun.*, 2024, **15**, 3524.
4. Z. Chang, G. Meng, Y. Chen, C. Chen, S. Han, P. Wu, L. Zhu, H. Tian, F. Kong, M. Wang, X. Cui and J. Shi, *Adv. Mater.*, 2023, **35**, 2304508.
5. G. Zhang, F. Wang, K. Chen, J. Kang and K. Chu, *Adv. Funct. Mater.*, 2024, **34**, 2305372.
6. L. Qiao, A. Zhu, D. Liu, K. An, J. Feng, C. Liu, K. W. Ng and H. Pan, *Adv. Energy Mater.*, 2024, **14**, 2402805.
7. H. Li, S. Li, R. Guan, Z. Jin, D. Xiao, Y. Guo and P. Li, *ACS Catal.*, 2024, **14**, 12042−12050.
8. M. Zheng, Y. Wan, Z.-H. Huang, F. Kang and R. Lv, *Adv. Mater.*, 2025, e14834.
9. Y. Wan, Y. Tang, Y. Zuo, K. Sun, Z. Zhuang, Y. Zheng, W. Yan, J. Zhang and R. Lv, *Energy Environ. Sci.*, 2025, **18**, 7460−7469.
10. X. Feng, J. Liu, Y. Kong, Z. Zhang, Z. Zhang, S. Li, L. Tong, X. Gao and J. Zhang, *Adv. Mater.*, 2024, **36**, 2405660.
11. K. Liu, H. Li, M. Xie, P. Wang, Z. Jin, Y. Liu, M. Zhou, P. Li and G. Yu, *J. Am. Chem. Soc.*, 2024, **146**, 7779−7790.